Acta Mech 214, 17–30 (2010)
DOI 10.1007/s00707-010-0308-7

Tatsuo Inoue

Tatara and the Japanese sword: the science and technology

Received: 5 May 2009 / Revised: 29 October 2009 / Published online: 5 June 2010

Abstract *Tatara*, a traditional steel-making system developed in Japan, and the Japanese sword are briefly introduced from a technological point of view, followed by some comments on scientific aspects. Attention is paid to the comparison with methods developed in foreign countries. The quenching process being operated in the final stage of sword making is focused on, and results of a computer simulation by a code COSMAP based on metallo-thermo-mechanics are presented to know how the temperature, metallic structure and stress/distortion vary in the process.

1 Introduction

So many monographs on the Japanese sword have been published in English [1–3] from the viewpoint of typical traditional crafts of arts. The sword is also interesting from the aspect of modern science and technology [4–7], since the way of making the Japanese sword is really consistent with science, like other surviving traditional products.

Most Japanese swords are made of characteristic and traditional Japanese steel, so-called *tamahagane*, but not of modern steel, produced by *tatara* system by use of iron sand. The author has so enjoyed to devote himself to accumulate information on the science of the Japanese sword-making and the *tatara* [8–23] and carried out some computer simulation in the course of quenching of the sword [24–35].

In the first part of this article, the author tries to show how to overview the swords by internet followed by the material and forging process of the Japanese sword with some comments. A special emphasis is placed on the computer simulation of quenching or hardening applied in the final stage of the manufacturing of the sword in the framework of continuum metallo-thermo-mechanics [36–46], representing the modes of the bending and the formation of the blade simulated mainly by a developed computer code "COSMAP" [47–50]. See http://homepage3.nifty.com/npo-mtm/, http://www.ideamap.co.jp.htm.

2 How to overview the *Tatara* and Japanese sword?

Over a million websites will be found for the keyword "sword", and almost half a million sites for "Japanese sword" in English and other language as well as in Japanese. The site and related links of Dr. L.A. Jones, http://www.vikingsword.com/noframes.html as well as http://www.myarmoury.com/home.html, are so brilliant and interesting, and we can obtain so many kinds of information. The site of Mr. Manabe, a sword master, http://www.eonet.ne.jp/~sumihira/, is interesting. Many kinds of movies are visible on the related site of http://jp.youtube.com/watch?v=R0DwAWut3b8&NR=1.

T. Inoue (✉)
High-Tech Research Center for Structural and Material Developments,
Fukuyama University, Gakuen-cho 1, Fukuyama, Japan
E-mail: inoue@fume.fukuyama-u.ac.jp; inoue@fuarc.fukuyama-u.ac.jp

There are many museums exhibiting swords. Readers are recommended to visit the Wallace Collection, London, http://www.the-wallace-collection.org.uk/, to see a lot of western medieval swords. The Society for Preservation of Japanese Art Swords and The Japanese Sword Museum, http://www09.u-page.so-net.ne.jp/rj8/nbthk-tk/, in Tokyo is one of the specialized museums of swords, and Wakou Museum, http://www.miraclewave.or.jp/yasugicity/alwakou.html, and Oku-izumo Tatara and Sword Museum, http://www.town.okuizumo.shimane.jp/tourist/guide/guide010/post-113.html, in Shimane. Bizen Osafune Japanese Sword Museum, http://www.city.setouchi.lg.jp/~osa-token/english/index.htm, as well as the site of Hitachi Metals, http://www.hitachi-metals.co.jp/e/index.html, provides information on *tatara*, the Japanese iron- and steel-making system.

As for the Japanese swords, Tawara, a professor of Japanese Sword Research Laboratory, the University of Tokyo, accomplished a monumental work in the framework of metallurgy [4]. Tawara measured the distribution of carbon density, precipitation and hardness in the cross-section of the swords in relation to the pattern of blade and *sori* representing the mode of deformation during quenching. Successive scientific works were made by Bain [5], Suzuki [6], Williams [10], Park [11], Sasaki [13], Shimura [14], Yamasue [17] and others.

Very few works on the sword are made, however, from a mechanical engineering aspect. Ishikawa–Yamada [15,16] discussed the mechanism of cutting objects from the theory of cutting, and the dynamics on sword-treating technique is analyzed by Daimaruya [18]. Stress and deformation analysis after quenching by the finite element method was carried out by Fujiwara–Hanabusa [8,9] and the present authors [24–35].

3 *Tamahagane* and the *Tatara* system

Due to the strength viewpoint, most surveying swords as weapons are made of steels, while copper and bronze swords were used for some purposes of decoration. As is well known, it is said that steels first appeared in Hittite at 23rd century B.C. The technology to produce steel from iron ore was transported to Europe, Asia and other areas in the world. The traditional steel in Japan, on the other hand, normally comes from iron sand processed in a special way, called *tatara* system (see Fig. 1). A popular Japanese animation movie "MONONOKE-HIME" or "PRINCESS-MONONOKE" treated the struggle of a human being who cut trees used for the fuel of *tatara* against the guardian god of the forest.

The Iron and Steel Institute of Japan constructed an experimental system of *tatara* in 1969 in Sugaya, Shimane Prefecture, and accumulated interesting data of steel-making technology. Due to the lack of steel for the sword, The Society for Preservation of Japanese Art Swords or the Nippon Bijutsu Token Hozon Kyokai started to organize the *tatara* system in Torigami, Shimane Prefecture, in the cooperation with Hitachi Metals, Ltd. in 1977 and provides several tons of steel every year.

Iron sand with 2–5% content of iron mined from mountains, which includes the best quality of iron sand in Japan, is concentrated to the degree of 50–60% by a magnet system, while the mineral dressing method by gravity classification in a flowing river, *kanna nagashi*, is no more popular due to water pollution problems. Such enriched iron sand called *masa satetsu* contains 8% of pure iron Fe and iron oxide Fe_2O_3 with a very small amount of impurities such as 0.026% P and 0.002% S being injurious for carbon steels. Here, alumina Al_2O_3 is so rare to be beneficial for low temperature refinement to be stated later.

Fig. 1 Old painting of *tatara*, traditional steel making system

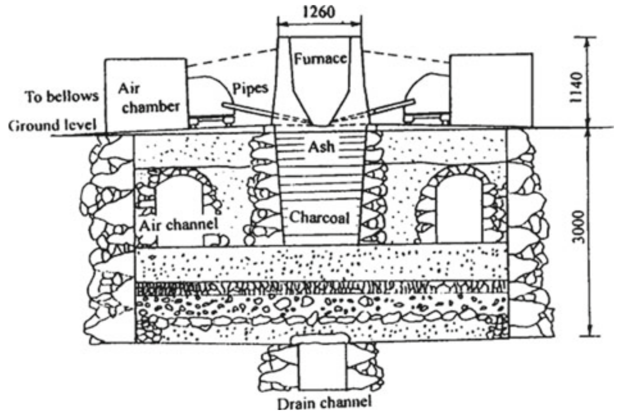

Fig. 2 Cross section of a *tatara* furnace

The enriched iron sand is supplied alternatively to the furnace with charcoal by hand. Figure 2 illustrates the cross-sectional view of the furnace under operation with a drainage mechanism constructed to three meters under the ground. The only difference of the system from the classical one in the figure is that electric motors are used for intermittent air blasts instead of manpowered bellows.

Continuous burning is operated for 70 h under the direction of a *murage* or chief foreman. The temperature in the furnace is around 1,200–1,500°C, lower than the melting point of the steel, which follows from the reduction process of the partly molten state occurring between iron oxide Fe_2O_3 and silica SiO_2 contained in the clay of furnace. During the process, the initial thickness of 200–400 mm of the furnace is reduced to 50–100 mm. After taking out the slag from the bottom of the furnace followed by destroying the whole system, an ingot of blister steel called *kera* in sponge state with dimension of 2.7 m in length, 1 m in width and 200–300 mm in thickness with a weight of 2–2.5 tons containing steel of 1.5–1.8 tons is obtained. Necessary amount of iron sand and charcoal are respectively 8 and 13 tons. (It is amazing that a *kera* costs hundred thousand dollars, over hundred times as expensive as modern steel!)

Steel produced on both sides of the *kera*, where enough deoxidization is accomplished by air blast from *kirokan* (special wooden pipes) is called *tamahagane* or noble steel, which is spelled as mother of metal in Japanese characters. Other parts of the block with different chemical composition are also used for the sword-making.

The chemical composition of the best part of the steel is 1.0–1.4% C, 0.02–0.03% P, 0.006% S and 0.003–0.004% Ti, being very rare of sulfur and phosphorus even compared with industrial carbon steel. The steel is cooled by the cold environment since the operation is carried out in the mid-winter and sheared into small pieces, and distributed to over 300 professional sword masters in Japan.

4 Manufacturing of a Japanese sword

The successive process of making a sword in a smith shop is illustrated in Fig. 3. The smith makes a flat plate with a handle termed as *tekoita,* on which the small pieces of broken flat pieces are piled up covered by a special Japanese paper dampened by water containing clay and ash of rice straws to prevent oxidation on the surface of steel by insulating air. The pieces of the steel with different carbon contents are heated in the forge in the carburizing or decarburizing environment, termed *jigane-oroshi*. This process is carried out in the forge burnt by charcoal with the blast air from *fuigo* (blower). Decarburization occurs in the part close to the blower, while CO_2 gas accelerates the sintering on the upper parts.

A block of steel heated up to 850–900°C is now forged and welded on the anvil by hammers sometimes operated by two or three people. Figures 4a and b respectively illustrate the forging process of a Japanese and western manner, which are principally similar. In the case of a Japanese sword, on the other hand, the sword smith folds the block about ten to fifteen rounds called *orikaeshi* to result in laminated materials with approximately 1,000 ($\approx 2^{10}$) to 30,000($\approx 2^{15}$) layers called *hada,* or skin, appearing as weld pattern on the surface of the sword. The characteristic pattern of the *hada*, representing laminated layers depending on the way of smiths is visible on the surface of the sword, some of which are depicted in Fig. 5. A similar weld pattern but created by twist welding is also seen in western swords as seen in Fig. 6. The pattern is observed

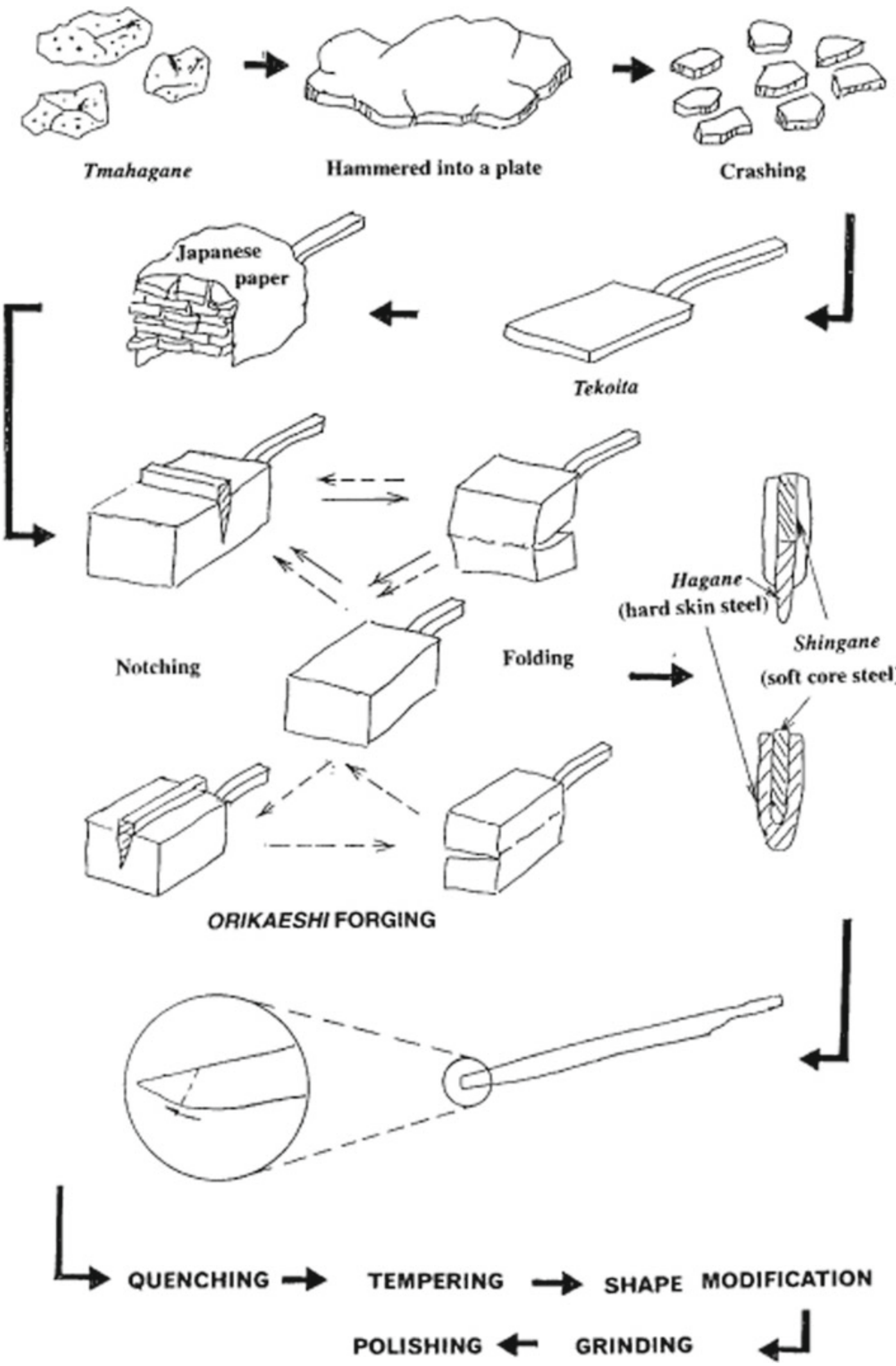

Fig. 3 Illustration of the manufacturing process of a Japanese sword

even in the western sword by Maeder [51] as seen in Fig. 7 if polished by a special Japanese technique, called *togi.*

Such bonding of layers during the repeated *orikaesi* and welding process is enhanced by the mechanism of so-called mechanical alloying, for which a very clean surface of the layers is necessary. This is achieved by dispersing impurities such as oxides and so on with sparks by hammering. The weight of the block decreases during the process to 700–1,000 g in the final shape of the Japanese sword being almost one half of the initial weight.

(a) (b)

Fig. 4 Similarity of forging operation. **a** Japanese style; **b** Western style

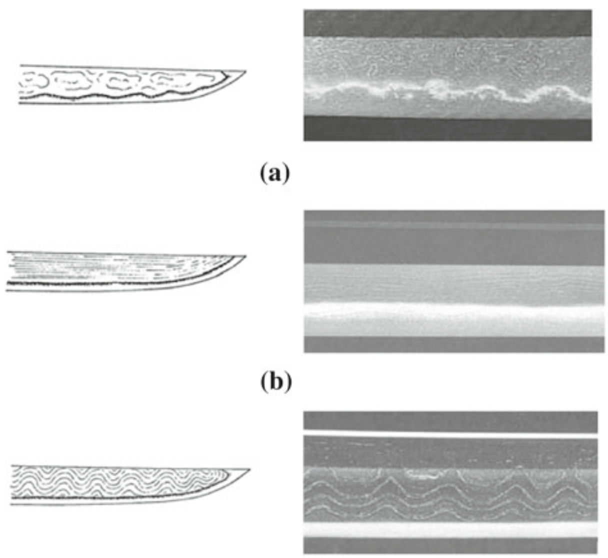

(a) (b) (c)

Fig. 5 *Hada*, weld patterns by forging with *hamon*, boundary of blade. **a** *Itame-hada*; **b** *Masame-hada*; **c** *Ayasugi-hada*

A bar of *shingane* (core steel) with low carbon content is covered by *kawagane* or *hagane* (skin steel) with high carbon for which the *tamahagane* steel is normally used (see the cross-sectional views in Fig. 3). This process is called *tsukurikomi*, a similarity can also be seen in European swords. This combination of two or three kinds of different steels with different carbon content induces the characteristic property of the sword with a sharp blade with enough ductility as a whole to absorb the bending moment during the cutting operation of obstacles. Such a combination of different kinds of steel results in the nonuniform distribution of carbon in the cross-section.

After rough shaping and grinding by the smith himself, the sword is transferred to the final process of *yakiire* (quenching or hardening), which is the main topic of numerical simulation in the following sections.

Before quenching or hardening, a kind of clay, *yakiba-tsuchi*, mixed with charcoal powder and so on is coated on the surface of the blade to control the heat transfer intensity in Fig. 8 to be discussed in the next section. The most interesting situation is that the coated clay is thick on the ridge (*mune*) while thin on the edge part (*hasaki*), which leads to an increase in the cooling rate of the edge part and so to deepen hardened depth. This clay-coating technique is employed for most blades of knives as well as swords, but is probably unique in Japan.

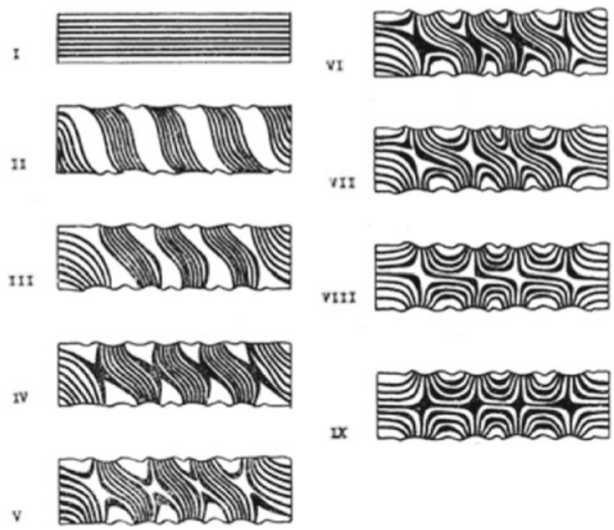

Fig. 6 Formation of weld pattern by twisting

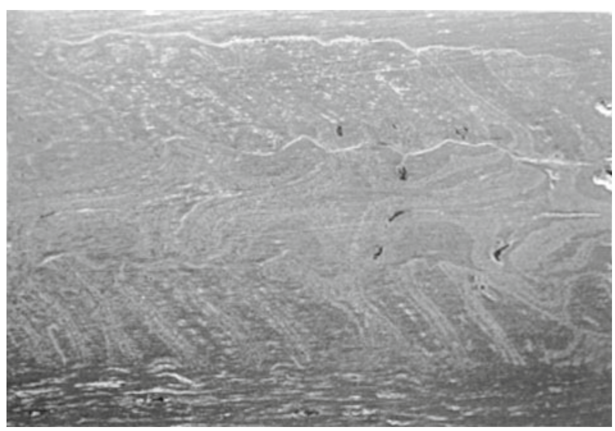

Fig. 7 Weld pattern in German sword

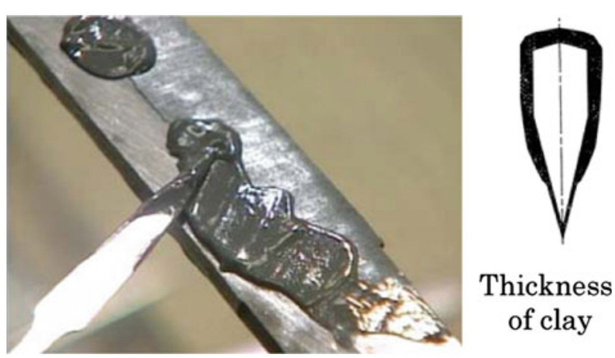

Fig. 8 Clay coating technique

Finally, the quenching operation of the sword heated up to 800–850°C into water is carried out. The maximum temperature of the heated sword and cooling water depend on the schools of smiths and the material properties as well as the dimension of the sword.

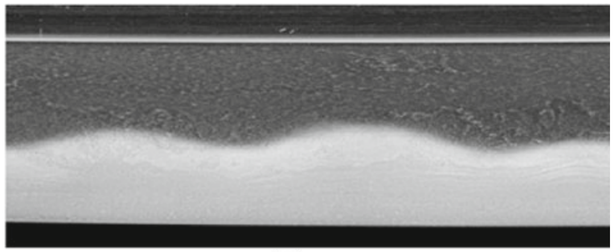

(a)

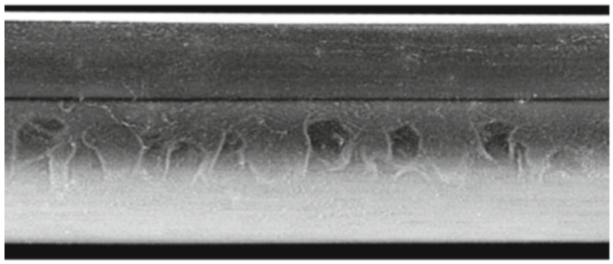

(b)

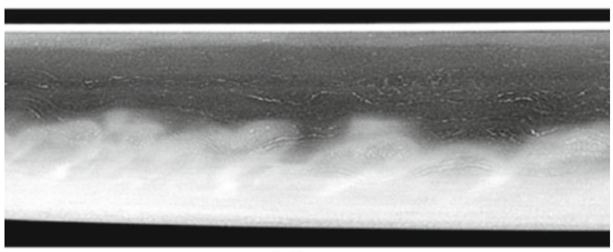

(c)

Fig. 9 Typical patterns of *hamon*. **a** *Gonome-midare*; **b** *Choji-midare*; **c** *Gyaku choji-midare*

During the quenching process, a white hard part with martensite structure is induced near the edge, while the other shining part remains pearlite and ferrite structure. The border of the parts is called *hamon*. Here, the wavy or zigzag pattern of the *hamon* is realized by cutting the clay with a spatula. This results in the variation of *hamon*, some of which are represented in Fig. 9.

5 Brief summary of metallo-thermo-mechanics and the developed CAE system "COSMAP"

In the course of quenching of the sword, or machine parts in general, incorporated with phase transformation, fields of metallic structure, temperature and stress/strain (deformation) are coupled to each other as schematically illustrated in the diagram of Fig. 10 [36].

The author has investigated the mechanics relevant to describing such three coupled fields for the last 30 years, being termed as metallo-thermo-mechanics, and recently tries to develop the data base MATEQ of many kinds of materials [52,53] necessary for the analysis. Each field is to be described by the coupled fundamental equations as follows [36–50,54–57]:

5.1 Mechanical constitutive equation

In most cases of phase transformation in solids occurring in the process of quenching, several constituents are induced to compose a material point so as to assume that the material point is a mixture of N kinds of phases. Denoting the volume fraction of the Ith constituent as ξ_I, the physical and mechanical properties χ of the material are assumed to be a linear combination of the properties χ_I of the constituents as

$$\chi = \sum_{I=1}^{N} \chi_I \xi_I \equiv \Sigma \chi_I \xi_I, \text{ with } \Sigma \xi_I = 1, \tag{1}$$

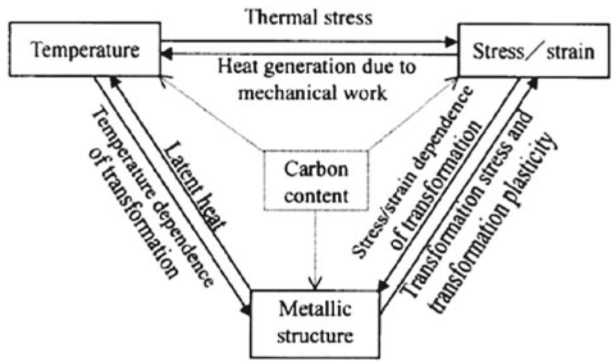

Fig. 10 Coupling among metallic structures, temperature and mechanical fields in the course of the heat-treating process

where $\Sigma_{I=1}^{N} \equiv \Sigma$ is the summation for suffix I from 1 to N. All material parameters appearing in the following are defined in the manner of Eq. (1).

To obtain an explicit expression for the elastic strain, the Gibbs free energy G is assumed to be determined by that of constituent G_I in the form of Eq. (1) as

$$G\left(\sigma_{ij}, T, \varepsilon_{ij}^{p}, \alpha_{ij}, \kappa, \xi_I\right) = \Sigma \xi_I G_I(\sigma_{ij}, T, \varepsilon_{ij}^{p}, \alpha_{ij}, \kappa). \tag{2}$$

Here, the back stress α_{ij} in the yield function F and the inelastic hardening parameter κ are regarded as internal variables. When G_I is divided into the elastic and inelastic parts as

$$G_I\left(\sigma_{ij}, T, \varepsilon_{ij}^{p}, \alpha_{ij}, \kappa, \xi_I\right) = G_I^{e}\left(\sigma_{ij}, T\right) + G_I^{p}\left(T, \varepsilon_{ij}^{p}, \alpha_{ij}, \kappa\right), \tag{3}$$

we can derive the elastic strain by expanding the elastic part G_I^e around the natural state, $\sigma_{ij} = 0$ and $T = T_0$, in terms of the representation theorem for an isotropic function:

$$\varepsilon_{ij}^{\mathrm{e}} = \left(\Sigma \frac{1+\nu_I}{E_I}\xi_I\right)\sigma_{ij} - \left(\Sigma \frac{\nu_I}{E_I}\xi_I\right)\delta_{ij}\sigma_{kk} + \delta_{ij}\int_{T_0}^{T} \Sigma \alpha_I \xi_I dT + \delta_{ij}\Sigma\beta_I(\xi_I - \xi_{I0}), \tag{4}$$

where E_I, ν_I, α_I and β_I correspond to Young's modulus, Poisson's ratio, thermal expansion coefficient and linear dilatation of the Ith constituent, respectively.

The evolution equation for unified plastic strain $\dot{\varepsilon}_{ij}^{p}$ including thermo-mechanical and transformation plastic parts is summarized to obtain the total strain rate with hardening modulus of the Ith phase $1/\hat{G}_I$ [54–56],

$$\begin{aligned} \dot{\varepsilon}_{ij}^{p} &= \sum_{I=1}^{N} \xi_I \dot{\varepsilon}_{Iij}^{p} \\ &= \sum_{I=1}^{N} \hat{G}_I \left[\left(\frac{\partial F_I}{\partial \sigma_{kl}}\xi_I\dot{\sigma}_{kl} + \frac{\partial F_I}{\partial T}\xi_I\dot{T}\right) + \xi_I\left(\sum_{N=1}^{\tilde{N}} \frac{\partial F_I}{\partial \zeta_J}\dot{\zeta}_J\right)\right]\frac{\partial F_I}{\partial \sigma_{ij}}. \end{aligned} \tag{5}$$

Here, a yield function for the Ith phase F_I is assumed to be affected by the growing new Jth phase with volume fraction ζ_J:

$$F_I = F_I\left(\sigma_{ij}, T, \varepsilon_{Iij}^{p}, \kappa_I, \zeta_J\right), \quad (I = 1, 2, \ldots, N;\ J = 1, 2, \ldots, M). \tag{6}$$

5.2 Heat conduction equation

Applying the Legendre transformation to the Gibbs free energy function (Eq. 2), the energy balance equation is reduced to the equation of heat conduction such that

$$\rho c\dot{T} - k\frac{\partial^2 T}{\partial x_i \partial x_i} + \rho\sum_{I=1}^{N} l_I \xi_I + T\frac{\partial \varepsilon_{ij}^{\mathrm{e}}}{\partial T}\dot{\sigma}_{ij} + \left(\rho\frac{\partial H}{\partial \varepsilon_{ij}^{i}}\dot{\varepsilon}_{ij}^{i} + \rho\frac{\partial H}{\partial s}\circ\dot{s} - \sigma_{ij}\dot{\varepsilon}_{ij}^{i}\right) = \rho\gamma, \tag{7}$$

where s denotes a set of scalar, vector or tensor internal variables with corresponding product $\circ$, and H and γ are respectively enthalpy density and heat generation. Then, the latent heat l_I due to the increase of the Ith phase is

$$l_I = \frac{\partial H}{\partial \xi_I}. \tag{8}$$

The fifth term on the left-hand side of Eq. (7) denotes the heat generation by inelastic dissipation, which is significant when compared with the elastic work represented by the fourth term, and the third term arises from the latent heat through phase changes. Hence, it can be seen that Eq. (7) corresponds to the ordinal equation of heat conduction, provided that these terms are neglected.

5.3 Kinetics of phase transformation

During phase transformation, a given volume of material is assumed to be composed of several kinds of constituent with the volume fraction ξ_I as expressed in Eq. (1). We choose three kinds of volume fraction: austenite ξ_A, pearlite ξ_P and martensite ξ_M, and other structures induced by precipitation by recovery effect, say during the annealing process. When austenite is cooled in equilibrium, bainite, ferrite and carbide are produced in addition to pearlite, but for brevity all these structures resulting from a diffusion type of transformation are called pearlite. The nucleation and growth of pearlite in an austenite structure are phenomenologically governed by the mechanism for a diffusion process, and Johnson and Mehl [58] proposed a formula for volume fraction ξ_P as

$$\xi_P = 1 - \exp\left(-V_{\mathrm{e}}\right), \tag{9}$$

where V_{e} means the extended volume of the pearlite given by

$$V_{\mathrm{e}} = \int_0^t \frac{4}{3}\pi R\left(t-\tau\right)^3 n\,\mathrm{d}\tau. \tag{10}$$

Here, R is the moving rate of the radius of the pearlite particle. Bearing in mind that the value of R is generally a function of stress as well as of temperature, Eq. (10) may be reduced to

$$V_{\mathrm{e}} = \int_0^t f\left(T, \sigma_{ij}\right)\left(t-\tau\right)^3 \mathrm{d}\tau. \tag{11}$$

The function $f(T, 0)$ can be determined by fitting the temperature–time transformation (TTT) diagram or continuous-cooling transformation (CCT) diagram without stress, and $f(T, \sigma_{ij})$ may be given by the start-time or finish-time data for pearlite transformation with an applied stress.

The empirical relationship for the austenite–martensite transformation is also obtainable by modifying the kinetic theory of Magee [59]. Assume that the growth of a martensite structure is a linear function of the increase in the difference ΔG in free energy between austenite and martensite as

$$\mathrm{d}\xi_M = -\bar{v}\left(1-\xi_M\right)\phi\,\mathrm{d}\left(\Delta G\right). \tag{12}$$

Regarding the Gibbs free energy G as a function of temperature and stress, we can obtain the form of ξ_M by integrating Eq. (12) as

$$\xi_M = 1 - \exp\left[\varphi_1\left(M_{\mathrm{s}} - T\right) + \varphi_2\left(\sigma_{ij}\right)\right]. \tag{13}$$

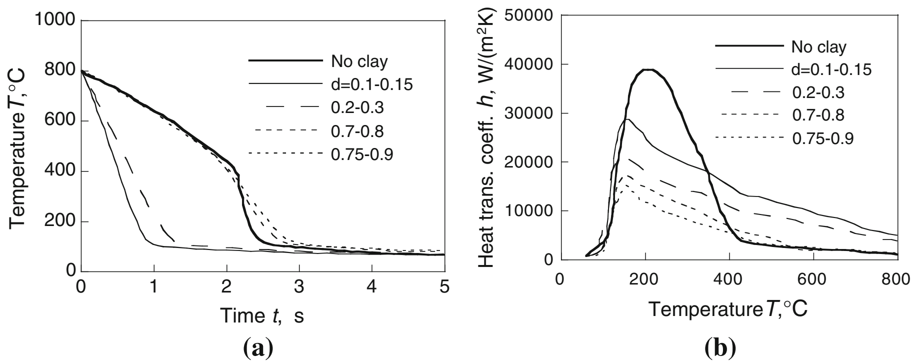

Fig. 11 Cooling curves depending on coated clay thickness. **a** Cooling curves depending on the thickness of clay; **b** Identified Heat transfer coefficient

The function $\varphi_2\left(\sigma_{ij}\right)$ is identified by the data subjected to applied stress.

Based on the metallo-thermo-mechanical theory, the authors developed a finite element CAE code 'HEARTS' for heat treatment [38,39] almost twenty years ago, which is now completely reproduced to 'COSMAP' [46–49]. The motivation of the author to devote himself to develop the codes rather comes from the hearty dream to simulate the coupled metallo-thermo-mechanical behavior of the Japanese sword during quenching.

6 Identification of heat transfer characteristics depending on clay pasting

Before quenching the Japanese sword into water, the *yakiba-tsuchi* clay is coated on the surface as shown in Fig. 8 to control the cooling condition of the surface of the steel. This kind of process to accelerate the cooling rate had been known by the sword smith since the method of manufacturing Japanese swords was established in the fifth or sixth century and is also applied to harden the blade of knives and other cutting tools. As far as the author knows, this kind of technique is specially developed in Japan.

Since the temperature distribution is to be calculated in the body of the sword, it is necessary to identify the relative heat transfer coefficient on the metal surface as the function of the thickness of the clay. Series of experiments based on Japan Industrial Standard, JIS-K2242, were made to measure the cooling curve of a cylinder made of silver coated by the clay with different thickness. A thermocouple is mounted on the surface. The cylinder is heated up to 800°C by a reflection type electric furnace and cooled in water.

Obtained cooling curves are demonstrated in Fig. 11a with the thickness of the pasted clay as parameter [24]. It is so interesting that the curves for thick clay (t = 0.7–0.8 and 0.75–0.9 mm) show typical mode with moderate cooling rate due to film boiling followed by severe cooling stage by nuclear boiling, the shape of which are similar to the case without the clay. When the thickness is small (t = 0.1–0.15 and 0.2–0.3 mm), on the other hand, no film boiling stage is observed, which means that the cylinder is cooled severely from the beginning. This is also confirmed by the observation of bubble nucleation by VTR. Inverse calculation is carried out by perturbation method to identify the heat transfer coefficient on the surface of the cylinder shown in Fig. 11b.

It is a paradox to be noted from Fig. 11b that the coefficient in the case with thin clay gives a higher value than the one without clay during 800-400°C, which is most important temperature range for quenching. (The mechanism of such a paradox is discussed by Kikuchi [60].) This data will be employed as the boundary condition when solving the coupled heat conduction equation [7].

7 Simulated results of the quenching process

Results of the simulation of a sword during the quenching process are briefly summarized in this section mainly by the code COSMAP. The data of the material are employed from the database MATEQ, and use is made of the heat transfer coefficient depicted in Fig. 11b.

7.1 Sword treated and the condition of simulation

The sword treated here is 500 mm in length with 7 mm in maximum width, which is a model of the author's classical sword made in the *Houki* region. A three-dimensional finite element mesh division of the sword is represented in Fig. 12, where the division is made for a half part in the width direction due to symmetry; and Fig. 12a and b, respectively, denotes the whole region and the enlarged part near the *kissaki* or tip. The total number of elements is 3,904 and that of the nodes is 5,205. This model is supposed to consist of two regions, core steel with 0.2% carbon content and skin steel with 0.65%C, to which different material data are applied.

To differentiate the relative heat transfer coefficient depending on the thickness of the *yakibatsuchi* clay, the surface of the sword is divided into two layers with different values as are evaluated by use of the cooling curves, also depending on temperature as depicted in Fig. 11b.

The sword is uniformly heated up to 850°C, at which temperature the whole region is changed into an austenitic structure, and the sword is quenched into water of 40°C.

7.2 Effect of the thickness of the pasted clay on the formation of *hamon*

To know the effect of the thickness of the clay on the induced *hamon* and the hardenability, simulation of quenching by use of different conditions of heat transfer coefficient, actually depending on the way of pasting of the clay, is carried out [24–35]. The red part of Fig. 13 represents the martensite-rich area while blue is the pearlite. Figure 13a is the simulated result when pasting thick clay on the entire region of the sword, which

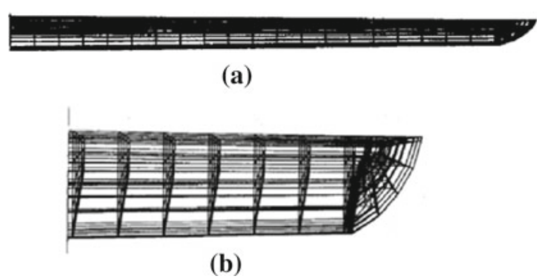

Fig. 12 Finite element division of the sword. **a** Entire region; **b** Near the tip

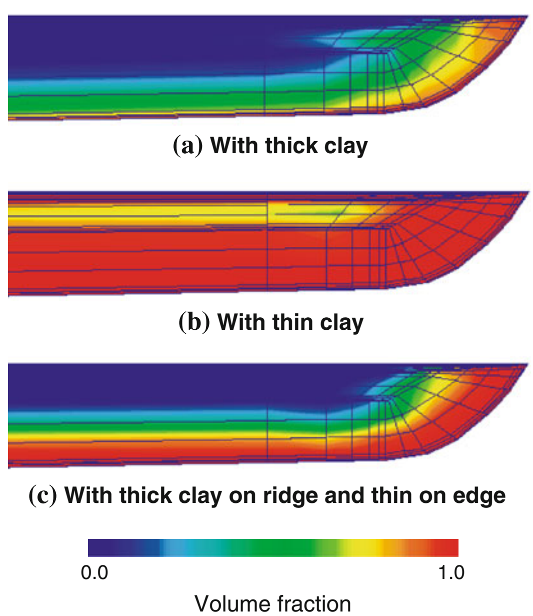

Fig. 13 Formation of hamon depending on the way of pasting clay

causes only a thin blade to be induced. Contrary to this, the whole region is covered by martensite when pasting thin clay as seen in Fig. 13b. The former sword might be ductile, but too soft on the edge for cutting, and the latter is too brittle. Figure 13c represents the proper distribution of martensite, with thick clay on the ridge and thin on the edge. It is surprising that old sword smiths knew such a way to control the clay thickness to obtain the proper distribution of *hamon*.

7.3 Variation of temperature, metallic structures and induced stress with association of deformation

The color in Fig. 14a demonstrates the temperature distribution of the surface of the sword with successive time from the beginning of quenching, and the mode of deformation is also depicted in the figure. Here, the clay is supposed to be pasted in the manner of Fig. 13c; thick on the ridge and thin on the edge.

The edge part of the sword with thin thickness shrinks due to thermal contraction by severe cooling, which leads to downward bending termed as *gyaku-sori* or reverse bending at $t = 1$ s. As seen in Fig. 14c, martensite starts to induce in the part, and volumetric dilatation causes the upward bending at 2 s, termed as *sori*. The second *gyaku-sori* is again observed at time $t = 1.5$ s since the ridge is converted from austenite to pearlite to cause the volumetric dilatation as represented in Fig. 14d. In the successive stage of cooling, the hot ridge side shrinks gradually because of thermal contraction, and finally, the normal bent shape can be obtained. Thus, simulated deformation gives good agreement with the actual bending mode of *sori*.

The pattern of stress distribution along the longitudinal direction is also depicted in Fig. 14b. In the mean time of the quenching operation, very high tensile stress occurs, which sometimes may lead to cracking or fracture of the sword. Residual stress in the final stage is in tension on the ridge while in compression on the edge, which is beneficial for reducing the bending stress during a cutting operation. The data of simulated residual stresses after complete cooling are compared with measured data by X-ray diffraction technique, and satisfactory coincidence is obtained [24,25].

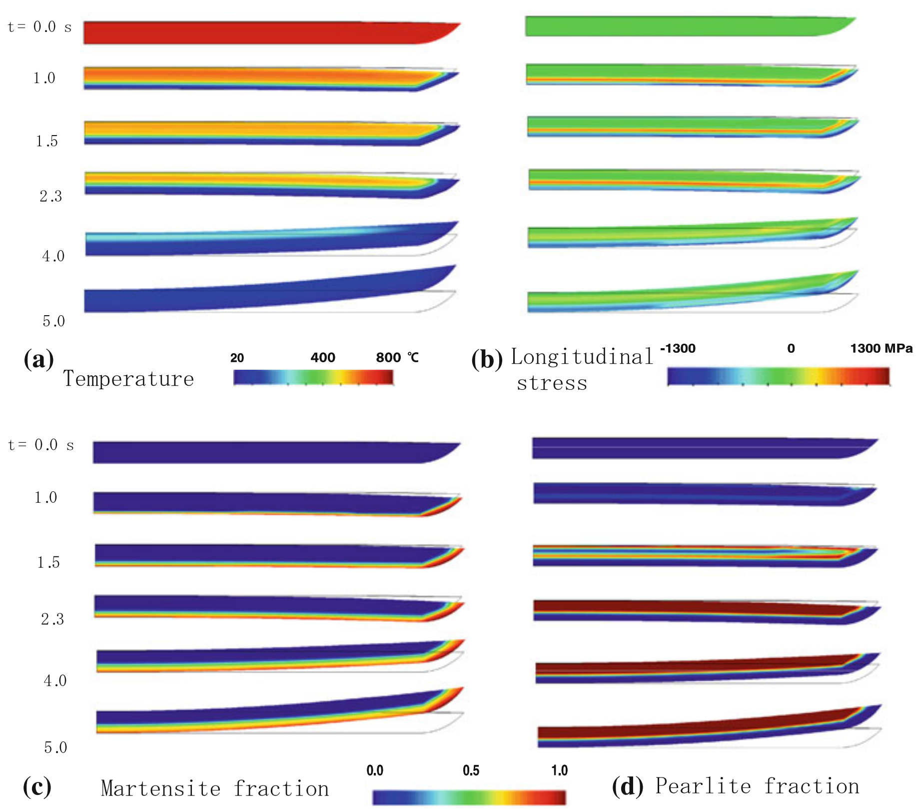

Fig. 14 Simulated results of variation of temperature, stress and phase distribution with distortion

8 Concluding remarks

The procedure of preparing the traditional Japanese steel, *tamahagane*, by the *tatara* system, and the method of manufacturing the Japanese sword are summarized from the scientific point of view. Here, the author's opinion related to the steel and sword-making process in foreign countries is stated.

As an example of the application of the simulation of quenching processes, a Japanese sword is focused, and the change in temperature, metallic structure and stress/deformation are calculated. The results reveal to represent real situations. The discussion from the viewpoints of metallurgy and mechanics are carried out in each section of preparing Japanese steel and manufacturing the sword, especially on the effect of pasted clay.

In conclusion, it is noted that the technology surviving for over thousand years is really consistent with modern science and technology. This means, on the other hand, that only technology based on scientific rationality can be successively transferred to the future.

Acknowledgments This Japanese sword project have been conducted for almost twenty years with the cooperation with my students to whom the author expresses his acknowledgment, especially Professor T. Uehara, now in Yamagata University, Mr. T. Ohtsuka, Nippon Steel Co., Mr. H. Kanamori, Idemitsu Kosan Co.. Illustrated simulation by COSMAP is carried out by Dr. R. Mukai, Saitama Institute of Technology, and photos of home-made swords taken by a scanner are kindly provided by Mr. S. Manabe, a sword master, a friend of the present author.

References

1. Kapp, L., Kapp, H., Yoshihara, Y.: The Craft of the Japanese sword. Kodansha International, Tokyo (1987)
2. Kanzan, K.: The Japanese Sword—A Comprehensive Guide. Kodansha International, Tokyo (1983)
3. Robinson, B.W.: The Arts of the Japanese Sword. Farber and Faber, London (1960)
4. Tawara, K.: Scientific Research on Japanese Swords (in Japanese). Hitachi-hyoronsha, Tokyo (1953)
5. Bain, B.C.: Nippon-to, an introduction of old swords of Japan. J. Iron and Steel Institute of Japan. 265–282 (1962)
6. Suzuki, T.: Traditional Technology of Making Japanese Swords (in Japanese). Rikougaku-sha, Tokyo (1994)
7. Ishikawa, K.: Nippon-Toh (Japanese Sword)—High-Technology Threading Through History, Lecture Note. Rochester Institute of Technology, Rochester (1993)
8. Fujiwara, H., Hanabusa, T.: Scientific research of Japanese sword—its curvature (sori) and residual stresses (in Japanese), Research Report, Faculty of Engineering, Tokushima University, 1 (1993)
9. Fujiwara, H., Hanabusa, T., Tanaka, K.: Scientific research of Japanese sword—its curvature (sori) and residual stresses. Proc. 3rd Int. Conf. Residual Stresses **2**, 1537–1542 (1991)
10. Williams, A.R.: Seven swords of the renaissance from an analytical point of view. Glaudius **14**, 97–127 (1978)
11. Inoue, T.: Tatara and the Japanese sword—-Advanced science and technology in the Japanese sword (in Japanese). Journal of the Japan Society of Mechanical Engineers. **97-903**, 132–135 (1998)
12. Park, J.S.: Traditional Japanese sword making from a tatara ingot from microstructural examination. ISIJ Int. **44-6**, 1040–1048 (2004)
13. Sasaki, N., Momono, T.: Change in carbon content of materials of the Japanese sword under traditional forging process. JISI Int. **93-12**, 792–798 (2007)
14. Matsumoto, K., Miyamoto, Y., Shimura, F.: Scientific connoisseur of a Japanese sword by minute impurity analysis. In: Proceedings of Annual Meeting of the Society for Scientific Studies of Cultural Properties (2006)
15. Yamada, H.: An engineering study on Nippon-Tou (in Japanese). J. Adv. Mach. **23-1**, 3–12 (2004)
16. Yamada, H., Sugita, T., Ishikawa, K.: A study of sharpness edge tool—2nd report; relation between cutting force and cutting condition. J. Adv. Mach. **19-1**, 49–53 (2000)
17. Yamasue, E.: Effect of size for tatara steelmaking furnace (in Japanese). Tetsu-to-Hagane **19-1**, 1–7 (2005)
18. Daimaruya, M., Kobayashi, H., Fujiki, H.: Impact Response of a model of a Japanese sword with Sori (in Japanese). In: Proceedings of 2006 Annual Meeting of JSME/MMD, pp.149–150 (2006)
19. Committee on Restoration Project of Tatara Steel-making System, Restoration of Tatara steelmaking process and the Blister steel (in Japanese), ISIJ-special report No. 9 (1970)
20. Matsushita, Y.: Restoration of the "Tatara" ironmaking process, an ancient ironmaking process of Japan (in Japanese). Proc. Int. Conf. Sci. Technol. Iron Steel Trans. ISIJ **11**, 212–218 (1971)
21. Kozuka, J.: "Tatara" process—a pig iron- and steel making process, transmitted from ancient times in Japan (in Japanese). Trans. ISIJ **8**, 36–47 (1968)
22. Kubota, K.: Japan's original steel making and its development under the influence of foreign technique (in Japanese). Coll. Int. Inst. CNRS, No.538 577–591 (1970)
23. Horikawa, K.: The ancient nails of "Horyuji" temple and the restoration of the "Tatara" ironmaking process (in Japanese). Bull. Metals Museum **12**, 29–37 (1982)
24. Uehara, T., Inoue, T.: Quenching process simulation of Japanese sword covered with clay (in Japanese). J. Soc. Mater. Sci. Japan **44**, 309–315 (1995)
25. Inoue, T.: Japanese sword in science and technology–computer simulation of quenching process (in Japanese). Boundary **11**, 36–41 (1995)
26. Inoue, T.: The Japanese sword—material, forging and simulation of quenching (in Japanese). Materia **135**, 174–178 (1996)

27. Inoue, T.: The Japanese sword—the material, manufacturing and computer simulation of quenching process. Mater. Sci. Res. Int. **3-4**, 193–203 (1997)
28. Inoue, T.: The Japanese sword—the material, manufacturing and computer simulation of quenching process, 2002. J. South African Arms and Armour Soc. 108–142 (2002)
29. Inoue, T.: Japanese sword in comparison with others. In: Proceedings of 8th International Conference on Mechanical Behaviour of Materials, pp. 458–468. Victoria, Canada, 16–21 May 1999
30. Inoue, T.: Science of Tatara and Japanese sword–traditional technology viewed from modern science. In: Proceedings of 1st International Conference on Business and Technology Transfer, pp. 131–138 (2002)
31. Inoue, T.: Scientific rationality in the Japanese sword (in Japanese). J. Japan Soc. Mech. Eng. **107-1027**, 132–135 (2004)
32. Inoue, T.: The science of Tatara and Japanese sword Part I (in Japanese). Kogyo-Kanetsu **42-2**, 5–11 (2005)
33. Inoue, T.: The science of Tatara and Japanese sword Part II (in Japanese). Kogyo-Kanetsu **42-3**, 3–9 (2005)
34. Inoue, T.: Science of Tatara and Japanese sword (in Japanese). In: Proceedings of 2006 Summer Conference, pp. 1–7. Soiety of Automotive Engineers of Japan (2006)
35. Inoue, T.: The Japanese sword—the art, comparison with foreign swords and metallo-thermomechanical simulation of quenching process (in Japanese). Materia **47-7**, 359–363 (2008)
36. Inoue, T., Nagaki, S., Kishino, T., Monkawa, M.: Description of transformation kinetics, heat conduction and elastic-plastic stresses in the course of quenching and tempering of some steels. Ing.-Archiv **50**, 315–327 (1981)
37. Inoue, T.: Metallo-thermo-mechanical coupling—application to the analysis of quenching, welding and continuous casting processes. Berg-Und Hutten-Mannische Monatshefte **132**, 63–71 (1987)
38. Inoue, T., Ju, D.Y., Arimoto, K.: Metallo-thermo-mechanical simulation of quenching process—theory, and implementation of computer code "HEARTS". In: Proceedings of 1st International Conference Quenching and Control of Distortion, pp. 205–212 (1992)
39. Inoue, T., Arimoto, K.: Development and implementation of CAE system "HEARTS" for heat treatment simulation based on metallo-thermo-mechanics. J. Mater. Eng. Perform. ASM **6-1**, 51–60 (1997)
40. Inoue, T.: Inelastic constitutive relationships and applications to some thermomechanical processes involving phase transformation, thermal stresses. In: Hetnarski, R.B. (ed.) vol. 3, pp. 1–20. North-Holland (1988)
41. Inoue, T., Wang, Z.G.: Metallo-thermo-mechanical simulation of some processes incorporating phase transformation, computational plasticity—current Japanese materials research. vol. 7, pp. 1–25. Elsevier Applied Science (1990)
42. Inoue, T.: Macro-, meso- and micro-scopic metallo-thermo-mechanics—application to phase transformation incorporating process simulation, Material Science Research International. 10-1, pp. 1–11 (2004-3)
43. Inoue, T.: Macro-, meso- and micro-scopic metallo-thermo-mechanics, J. de Physique V. **120**, 3–20 (2004-12)
44. Inoue, T.: Makro-Mezo-i Mikroskopowe Sposoby Oceny Przemian Fazowych w Metalach Uwzgled-najace Proces Symulacji Komputerowej. Inzynieria Powierzchni, Nr **1**, 23–35 (2005)
45. Inoue, T.: Metallo-thermo-mechanics—application to quenching, Handbook of Residual Stress and Distortion in Steel (Coedited by Totten, G., Morse H., Inoue, T.) ASM-International, pp. 296–311 (2002)
46. Inoue, T.: Thermal-metallurgical-mechanical inter-actions during welding, progress and mechanism of welding residual stress and distortion In: Feng, Z. (ed.) Woodhead Publishing Ltd. pp. 99–125 (2005-11)
47. Ju, D.Y., Ito, Y., Inoue, T.: Simulation and verification of residual stresses and distortion in carburized-quenching process of a gear shaft. In: Proceedings of 4th International Conference on Quenching and the Control of Distortion, pp. 291–296. Beijing 20–23 May 2003
48. Ju, D.Y., Inoue, T.: On the material process simulation code COSMAP—simulation examples and its experimental verification for heat treatment process. Key Eng. Mater. **345-346**, 955–958 (2007)
49. Ju, D.Y., Ito, Y., Inoue, T.: Simulation and experimental verification of carburized and nitrided quenching process. In: Proceedings of 3rd International Conference on Thermal Process Modelling and Simulation, Budapest (2006-5)
50. Ju, D.Y., Inoue, T.: Simulation and its experimental verification by a material process CAE code COSMAP. In: International Journal of Microstructure and Materials Properties (in press)
51. Maeder, S.: Stähle, Steine und Schlangen—Ein Beitrag zur Kulturgeschichte von Schwertklingen des frühen Mittelalters. Dissertation zur Enlangung des Doktorgrades der philosophischen Fukurtaten der Himboldt Universitat zu Berlin, 2001 (PhD-thesis), p. 340. Berlin (2001)
52. Inoue, T., Okamura, K.: Material database for simulation of metallo-thermo-mechanical fields. In: Proceedings of 5th International Symposium on Quenching and Distortion Control, pp.753-760. ASM, St. Louis (2000)
53. Subcommittee on Material Database, Committee on Engineering Plasticity, Materials database for simulation of metallo-thermo-mechanical fields (in Japanese). J. Mater. Sci. Japan. **51–3**, 350–355 (2002)
54. Inoue, T.: Unified transformation-thermoplasticity and the application (in Japanese). J. Soc. Mater. Sci. Japan **56–4**, 352–356 (2007)
55. Inoue, T.: Phenomenological mechanism of transformation plasticity and the constitutive law coupled with thermo-mechanical plasticity. Adv. Mater. Res. **33–37**, 1351–1358 (2008)
56. Inoue, T.: Mechanism of transformation plasticity and the unified constitutive equation for transformation-thermo-mechanical plasticity with some applications. In: Proceedings of 2nd International Conference on Distortion Engineering, pp. 441–450. Bremen (2008)
57. Tanaka, T., Inoue T.: Identification of trans-formation plasticity coefficient for some steels during pearlite transformation and the dependence on chemical composition (in Japanese). J. Soc. Mater. Sci. Japan. 56–10 (2008) pp. 1036–1042
58. Johnson, W.A., Mehl, R.F.: Reaction kinetics in processes of nucleation and growth. Trans. AIME **135**, 416–458 (1939)
59. Magee, C.L.: The Nucleation of Martensite, Ch.3, ASM (1968)
60. Kikuchi, Y.: The effect of thin coating material on rapid cooling of hot metal in boiling liquid. Netsu Shori **46–6**, 359–366 (2006)